Mattia Albiero,[1] Nicol Poncina,[1,2] Marc Tjwa,[3] Stefano Ciciliot,[1,2] Lisa Menegazzo,[1,2] Giulio Ceolotto,[2] Saula Vigili de Kreutzenberg,[2] Rute Moura,[3] Marco Giorgio,[4] Piergiuseppe Pelicci,[4] Angelo Avogaro,[1,2] and Gian Paolo Fadini[1,2]

Diabetes Causes Bone Marrow Autonomic Neuropathy and Impairs Stem Cell Mobilization via Dysregulated *p66Shc* and *Sirt1*

Diabetes compromises the bone marrow (BM) microenvironment and reduces the number of circulating CD34$^+$ cells. Diabetic autonomic neuropathy (DAN) may impact the BM, because the sympathetic nervous system is prominently involved in BM stem cell trafficking. We hypothesize that neuropathy of the BM affects stem cell mobilization and vascular recovery after ischemia in patients with diabetes. We report that, in patients, cardiovascular DAN was associated with fewer circulating CD34$^+$ cells. Experimental diabetes (streptozotocin-induced and *ob*/*ob* mice) or chemical sympathectomy in mice resulted in BM autonomic neuropathy, impaired Lin$^-$cKit$^+$Sca1$^+$ (LKS) cell and endothelial progenitor cell (EPC; CD34$^+$Flk1$^+$) mobilization, and vascular recovery after ischemia. DAN increased the expression of the 66-kDa protein from the src homology and collagen homology domain (*p66Shc*) and reduced the expression of sirtuin 1 (*Sirt1*) in mice and humans. *p66Shc* knockout (KO) in diabetic mice prevented DAN in the BM, and rescued defective LKS cell and EPC mobilization. Hematopoietic *Sirt1* KO mimicked the diabetic mobilization defect, whereas hematopoietic *Sirt1* overexpression in diabetes rescued defective mobilization and vascular repair. Through *p66Shc* and *Sirt1*, diabetes and sympathectomy elevated the expression of various adhesion molecules, including *CD62L*. *CD62L* KO partially rescued the defective stem/progenitor cell mobilization. In conclusion, autonomic neuropathy in the BM impairs stem cell mobilization in diabetes with dysregulation of the life-span regulators *p66Shc* and *Sirt1*.

Diabetes 2014;63:1353–1365 | DOI: 10.2337/db13-0894

Diabetes reduces the availability of bone marrow (BM)-derived circulating angiocompetent CD34$^+$ cells, especially in the presence of chronic vascular complications (1,2). This is believed to represent a risk factor for adverse outcomes, as a low CD34$^+$ cell count is associated with incident cardiovascular events (3). Recently, the BM has emerged as a previously neglected target of hyperglycemic damage in experimental and human diabetes, with features of microangiopathy and niche dysfunction (4–7). As a result of BM remodeling, mobilization of

[1]Venetian Institute of Molecular Medicine, Padova, Italy
[2]Department of Medicine, University of Padova, Padova, Italy
[3]Laboratory Vascular Hematology/Angiogenesis, Institute for Transfusion Medicine, Goethe University Frankfurt, Frankfurt, Germany
[4]European Institute of Oncology, Italian Foundation for Cancer Research Institute of Molecular Oncology-European Institute of Oncology Campus, Milan, Italy

Corresponding author: Gian Paolo Fadini, gianpaolofadini@hotmail.com or gianpaolo.fadini@unipd.it.

Received 7 June 2013 and accepted 15 November 2013.

This article contains Supplementary Data online at http://diabetes.diabetesjournals.org/lookup/suppl/doi:10.2337/db13-0894/-/DC1.

See accompanying article, p. 1185.

stem and progenitor cells is impaired in diabetic animals and humans (7–10). Since mobilization of BM-derived stem/progenitor cells contributes to angiogenesis and endothelial repair (11,12), such stem cell "mobilopathy" (13) is expected to promote cardiovascular disease in diabetes.

The sympathetic nervous system (SNS) is prominently involved in BM niche function (14) and stem cell trafficking is regulated by catecholaminergic neurotransmitters (15,16). Recently, it has also been demonstrated that BM denervation strongly contributes to chemotherapy-induced myelotoxicity (17). Diabetic patients often experience autonomic neuropathy, which is characterized by pauperization of SNS fibers in multiple organs (18–20). Thus, we herein hypothesize that diabetic autonomic neuropathy (DAN) can affect BM function and stem cell mobilization. Starting from the observation that patients with DAN have a marked pauperization of peripheral blood (PB) $CD34^+$ cells, we used several experimental models and conditions to demonstrate that autonomic neuropathy in the BM is causally linked to impaired stem cell mobilization in diabetes, which is associated with defective reperfusion after ischemia. Our data show that denervation in the diabetic BM is mediated by the 66-kDa protein from the src homology and collagen homology domain (*p66Shc*) and that impaired mobilization relies on sirtuin 1 (*Sirt1*) dysregulation, both of which are therefore potential targets to restore BM cell–mediated vascular repair.

RESEARCH DESIGN AND METHODS

Patients

The protocol was approved by the Ethics Committee of the University Hospital of Padova, and experiments were conducted in accordance with the Declaration of Helsinki, as revised in 2000. Patients were recruited at the diabetes outpatient clinic of the University Hospital of Padova. All consecutive type 1 diabetes (T1D) or type 2 diabetes (T2D) patients aged 20–90 years and undergoing autonomic neuropathy tests were eligible, provided they were clinically stable and free from exclusion criteria (recent acute disease or infection, trauma, or surgery; uncontrolled hypertension or hyperglycemia, prevalent hypoglycemia; immunological disorders, organ transplantation, or immunosuppression; pregnancy and lactation). The following data were recorded: age, sex, type of diabetes and disease duration, HbA_{1c} level, BMI, waist circumference, smoking habit, systolic and diastolic blood pressure, history of hypertension and use of antihypertensive medications, resting heart rate, lipid profile, albumin/creatinine excretion ratio, diabetes complications, and medications. Diabetic nephropathy was defined as a urinary albumin/creatinine ratio >30 mg/g or an estimated glomerular filtration rate <60 mL/min/1.73 m^2. Coronary artery disease was defined as a history of myocardial infarction or angina, confirmed by coronary artery angiography or a myocardial stress test. Peripheral arterial disease was defined as a history of claudication or rest pain with evidence of stenosis of leg arteries upon invasive or noninvasive examination. Cerebrovascular disease was defined as a history of stroke or evidence of >30% carotid stenosis upon ultrasound examination. Diagnosis of DAN was performed according to standard interpretation of R-R interval variations during a change from lying to standing, deep breathing, and Valsalva maneuver, as well as according to the degree of orthostatic hypotension. Age-specific thresholds were used to define pathological vs. normal DAN tests.

Animals

All procedures were approved by the local ethics committee and from the Italian Ministry of Health. Experiments were conducted according to the National Institutes of Health *Principles of Laboratory Animal Care*. *Vav1-Sirt1*$^{-/-}$ (generated by crossing *Vav1*$^{cre/+}$ mice with *Sirt1*$^{stop\text{-}flox}$ mice), *Vav1-Sirt1*^{TG} (generated by crossing *Vav1*$^{cre/+}$*Sirt1*$^{ex4.\Delta flox/+}$ with *Sirt1*$^{ex4.flox/flox}$), and *Vav1-YPF* mice were bred at the external mouse facilities of the University of Frankfurt (mfd Diagnostics GmbH). *Sell*$^{-/-}$ mice were bred at the mouse facilities of the Institut für Labortierkunde, University of Zurich (Zurich, Switzerland). *Sell*$^{-/-}$ mice were generated by Richard Hynes, a Howard Hughes Medical Institute Investigator at the Massachusetts Institute of Technology (Cambridge, MA). *p66Shc*$^{-/-}$ and *ob/ob p66Shc*$^{-/-}$ animals were bred at the animal facility of the University of Padova. The *ob/ob* mice were from The Jackson Laboratory (Bar Harbor, ME). Age-matched wild-type animals were obtained from the in-house colony of the animal facility of the Venetian Institute of Molecular Medicine (Padova, Italy). All animals were on a C57BL/6 background. Diabetes was induced with a single intraperitoneal injection of 150 mg/kg streptozotocin (STZ) (Sigma-Aldrich, St. Louis, MO) in citrate buffer 50 mmol/L, pH 4.5. Blood glucose was measured with Glucocard G-meter (Menarini, Florence, Italy); animals with blood glucose levels ≥300 mg/dL in at least two measurements within the first week were classified as diabetic and were housed for 4 weeks with feeding and drinking ad libitum before performing experiments. In a separate set, animals were killed at week 1, 2, and 3 after STZ treatment for a time-course analysis (n = 4–5/group). For SNS disruption, animals received three intraperitoneal injections of 100 mg/kg 6-hydroxydopamine (6-OHDA; Tocris Bioscience, Bristol, UK), which destroys sympathetic neurons through oxidative stress and other mechanisms. Animals were housed for 4 weeks before a second round of injections with two doses of 6-OHDA (100 mg/kg on day 0, 250 mg/kg on day 2), and experiments were started on day 5.

Hind-Limb Ischemia

Animals were sedated with 10 mg/kg zolazepam/thylamine (Zoletil; Virbac, Nice, France) and 7 mg/kg xylazine (Xilor; Bio98 Srl, Milan, Italy). The femoral artery

and the vein were surgically dissected from the femoral nerve, then cauterized with low-temperature cautery, and excised between inguinal ligament and hackle. Fifteen days after surgery, we measured hind-limb microvascular perfusion with the Periscan-Pim II Laser Doppler System (Perimed AB, Järfälla, Sweden). Each measure was repeated five times.

Mobilization Assays and Flow Cytometry

Progenitor cell levels were quantified in PB after peripheral ischemia or after 4 days of subcutaneous injection of 200 μg/kg/day human recombinant granulocyte colony-stimulating factor (G-CSF) (Filgrastim; Roche, Basel, Switzerland). Based on a preliminary analysis of the kinetics of endothelial progenitor cells (EPCs) and $Lin^{-}cKit^{+}Sca1^{+}$ (LKS) cells after ischemia, EPC levels peaked at day 3 after ischemia, and LKS cell levels peaked at day 14. Therefore, these time points were used for all subsequent analyses. AMD3100 (Tocris Bioscience) was administered intraperitoneally at 6 mg/kg, and mobilization was assessed after 4 h. Desipramine treatment (10 mg/kg i.p.; Tocris Bioscience) was started 4 days before G-CSF treatment and continued for the 4 days of G-CSF treatment. PB was collected at baseline and after mobilization. One hundred fifty microliters of PB was stained with a rat anti-mouse allophycocyanin lineage cocktail (BD, Franklin Lakes, NJ), phycoerythrin rat anti-mouse Sca-1 (Ly6A/E; BD) and fluorescein isothiocyanate rat anti-mouse cKit (BD) to quantify LKS cells or with Alexa Fluor 647 rat anti-mouse CD34 (BD) and Alexa Fluor 488 anti-mouse Flk-1 (BioLegend, San Diego, CA) to quantify endothelial-committed progenitors. CD62L (L-selectin) expression on BM LKS cells was performed by staining 10^6 nonfractioned BM cells with LKS antibodies and PerCp Cy5.5 anti-Mouse CD62L (BD). A total of 250,000 events were acquired for each analysis, and the level of progenitor cells was expressed as the number of positive events per 1,000,000 total events. Data were acquired using a FACSCalibur instrument (BD Biosciences, San Jose, CA) and analyzed with FlowJo X (Tree Star Inc., Ashland, OR). For quantification of circulating stem cells in humans, we stained 150 μL of freshly collected PB with a phycoerythrin-conjugated anti-human CD34 monoclonal antibody (BD) and gated $CD34^{+}$ cells in the mononuclear cell fraction. $CD34^{+}$ cell count was expressed either as the number of events per 10^6 total events or cells per milliliter by multiplying the fractional $CD34^{+}$ cell count by white blood cells obtained from the automated hemocytometer.

Histology

Adductor femoris longus muscles were frozen in isopentane cooled in liquid nitrogen immediately after dissection. Muscles were then stored at −80°C for further analysis. Muscle sections were incubated with a DyLight594-conjugated Isolectin B4 (*Bandeiraea simplicifolia*, 1:100; Vector Laboratories) and costained with Oregon Green–conjugated wheat-germ agglutinin (1:400; Invitrogen) to allow identification of capillaries and muscle fibers. Nuclei were counterstained with Hoechst 33258 (Sigma-Aldrich). Femurs were fixed for 24 h in 4% paraformaldehyde at 4°C, washed with PBS, and then decalcified by incubation with 5% formic acid for 2 days at 4°C. Demineralized femurs were then covered with OCT embedding medium and frozen in liquid nitrogen. Ten-micrometer-thick longitudinal femur or transversal muscle sections were obtained with a Leica CM1950 cryostat. Femur sections were fixed in 4% paraformaldehyde and incubated with tyrosine hydroxylase antibody overnight at 4°C (rabbit polyclonal antibody, 1:100, AB152; Millipore). A mock incubation, without primary antibody, was performed in parallel. Images were acquired with a Leica DM5000B microscope equipped with a Leica DFC300 FX charge-coupled device camera, and were processed with ImageJ software (National Institutes of Health). Ten random ×20 magnification pictures were obtained from each muscle sample.

In Vitro Experiments

Human PB mononuclear cells (PBMCs) were obtained from healthy donors and separated by gradient centrifugation with Histopaque-1077 (Sigma-Aldrich). A total of 10^7 cells/well were plated in a six-well culture plate (BD) with RPMI 1640 medium supplemented with 10% FBS and 1% penicillin/streptomycin/glutamine. Isoproteronol (Sigma-Aldrich) was added for 48 h. Then cells were collected and lysed for gene expression analysis. To test chemical toxicity, BM cells from control mice were incubated for 1 h with STZ and 6-OHDA, followed by 24 h of recovery at 37°C 5% CO_2 with RPMI 1640 supplemented with 10% FBS and 1% penicillin/streptomycin/glutamine, at concentrations that are supposed to be achieved in vivo in mice. Live early and late apoptotic and necrotic cells (total BM cells or gated $CD34^{+}$ cells) were quantified by flow cytometry staining with propidium iodide and Annexin-V (BD). Hematopoietic colonies were grown from unfractioned BM cells and quantified using the MethoCult system (StemCells Inc., Vancouver, BC, Canada).

Molecular Biology

After mice were killed, bones were harvested, cleaned of debris, and flushed with ice-cold PBS; cells were collected through a 40-μm sterile filter, total RNA was extracted using the RNeasy kit (Qiagen), and RNA was quantified using a Nanodrop Spectrometer (Thermo Fisher Scientific). Four hundred nanograms of RNA were reverse-transcribed to cDNA using the First-Strand cDNA Synthesis Kit (Invitrogen). Duplicates of sample cDNA were then amplified on the 7900HT Fast Real-Time PCR System (Applied Biosystems) using the Fast SYBR Green RT-PCR kit (Applied Biosystems) in 96-well plates (Applied Biosystems). Expression data of selected genes were normalized against housekeeping genes and were analyzed using the $2^{(-\Delta\Delta ct)}$ method. Primer sequences are reported in Supplementary Table 3.

Statistical Analysis

Data are expressed as the mean ± SE or percentage. Comparison between two or more groups was performed using Student *t* test or ANOVA (for normal variables), and with Mann-Whitney *U* test and Kruskal-Wallis test (for non-normal variables). For human studies, a multivariable analysis was run to detect the independent effect of DAN: the $CD34^+$ cell count was the dependent variable, and clinical characteristics that were different at univariate analysis in Table 1 were explanatory independent variables. Statistical significance was accepted at $P < 0.05$.

RESULTS

Autonomic Neuropathy Impairs BM Stem Cell Mobilization in Diabetes

First, we found that the coexistence of multiple pathologic cardiovascular autonomic tests used to diagnose DAN was associated with a progressive reduction of $CD34^+$ cells in PB of diabetic patients (Fig. 1*A* and *B*). Independent of confounders, patients with DAN had a 40% reduction in PB $CD34^+$ cells compared with DAN-free patients (Fig. 1*C* and *D*, Table 1, and multivariate analysis in Supplementary Table 1). A breakdown analysis by DAN test showed trend reductions of PB $CD34^+$ cells in the presence of the alteration of each of the autonomic function tests (Fig. 1*E* and *F*). These data suggest that autonomic neuropathy in diabetic patients reduces the number of circulating $CD34^+$ cells, which have been previously shown to exert proangiogenic activity in vivo (21), that their levels are informative of the BM status (8) and predict future cardiovascular events (22).

Next, we report that experimental T1D induced by STZ caused a marked reduction in tyrosine-hydroxilase$^+$ ($Tyr\text{-}OH^+$) SNS fibers in the BM. This was equal to ~80% of Tyr-OH staining reduction obtained by chemical sympathectomy with 6-OHDA. STZ is considered to exert little or no myelosuppression because it enters the cells via glucose transporters (23). However, to rule out that BM sympathectomy was attributable to STZ toxicity and not to diabetes, we analyzed BM Tyr-OH staining in *ob/ob* mice, a model of T2D, and found a similar pauperization of SNS fibers (Fig. 2).

To test the consequence of sympathectomy on BM function in diabetes, we analyzed LKS cells and $CD34^+Flk1^+$ cells (EPCs) in T1D mice and 6-OHDA–treated mice before and after stimulation with G-CSF or hind-limb ischemia. Consistent with previous findings (8), diabetic animals were unable to mobilize LKS cells and EPCs after G-CSF or ischemia. Mice treated with 6-OHDA also showed impaired mobilization of LKS cells and EPCs in response to both stimuli (Fig. 3*A* and *B*). While the SNS dependency of the mobilizing effect of G-CSF is well-established (14), the role of BM SNS in ischemia-induced mobilization was hitherto unknown. The BM content of EPCs, but not of LKS cells, was reduced in

Table 1—Clinical characteristics of the study population

Characteristics	No DAN (*n* = 112)	DAN (*n* = 29)
Age (years)	59.1 ± 11.1	52.2 ± 13.8*
Sex male	66	59
T1D/T2D	24/88	12/17*
Diabetes duration (years)	10.5 ± 9.9	12.0 ± 10.2
HbA_{1c} (%)	7.7 ± 1.5	8.8 ± 2.1*
BMI (kg/m^2)	28.6 ± 5.4	27.7 ± 5.4
Waist circumference (cm)	94.6 ± 26.7	92.8 ± 24.7
Smoking habit	14	14
Hypertension	61	66
Systolic blood pressure (mmHg)	131.7 ± 16.8	130.2 ± 18.5
Diastolic blood pressure (mmHg)	78.5 ± 10.2	77.8 ± 8.4
Heart rate (bpm)	74.9 ± 10.7	80.3 ± 12.0*
Total cholesterol (mg/dL)	181.9 ± 41.3	179.4 ± 56.1
HDL cholesterol (mg/dL)	50.7 ± 17.1	48.2 ± 20.6
LDL cholesterol (mg/dL)	108.9 ± 28.8	110.3 ± 35.8
Triglycerides (mg/dL)	121.5 ± 81.0	123.0 ± 64.7
Coronary artery disease	7	10
Peripheral arterial disease	8	7
Cerebrovascular disease	38	45
Retinopathy	19	55*
Serum creatinine (μmol/L)	72.6 ± 28.2	83.2 ± 25.9
Albumin excretion rate (mg/g)	63.7 ± 274.6	167.5 ± 358.5
Albumin excretion rate >30 mg/g	26.8	44.8
Insulin	38	57
Metformin	51	43
Sulphonylureas	17	11
Glinides	4	4
Glitazones	3	7
DPP-4 inhibitors	8	4
GLP-1 receptor agonists	1	0
ACEi/ARBs	63	54
Calcium antagonists	15	14
β-Blockers	17	18
Aspirin	29	32
Statin	60	54
Fibrate	4	0
$CD34^+/10^6$ cells	464 ± 203	279 ± 174

Data are mean ± SE or %, unless otherwise indicated. DPP-4, dipeptidyl peptidase-4; GLP-1, glucagon-like peptide 1; ACEi, angiotensin-converting enzyme inhibitor; ARB, angiotensin receptor blocker. *$P < 0.05$, DAN vs. no DAN.

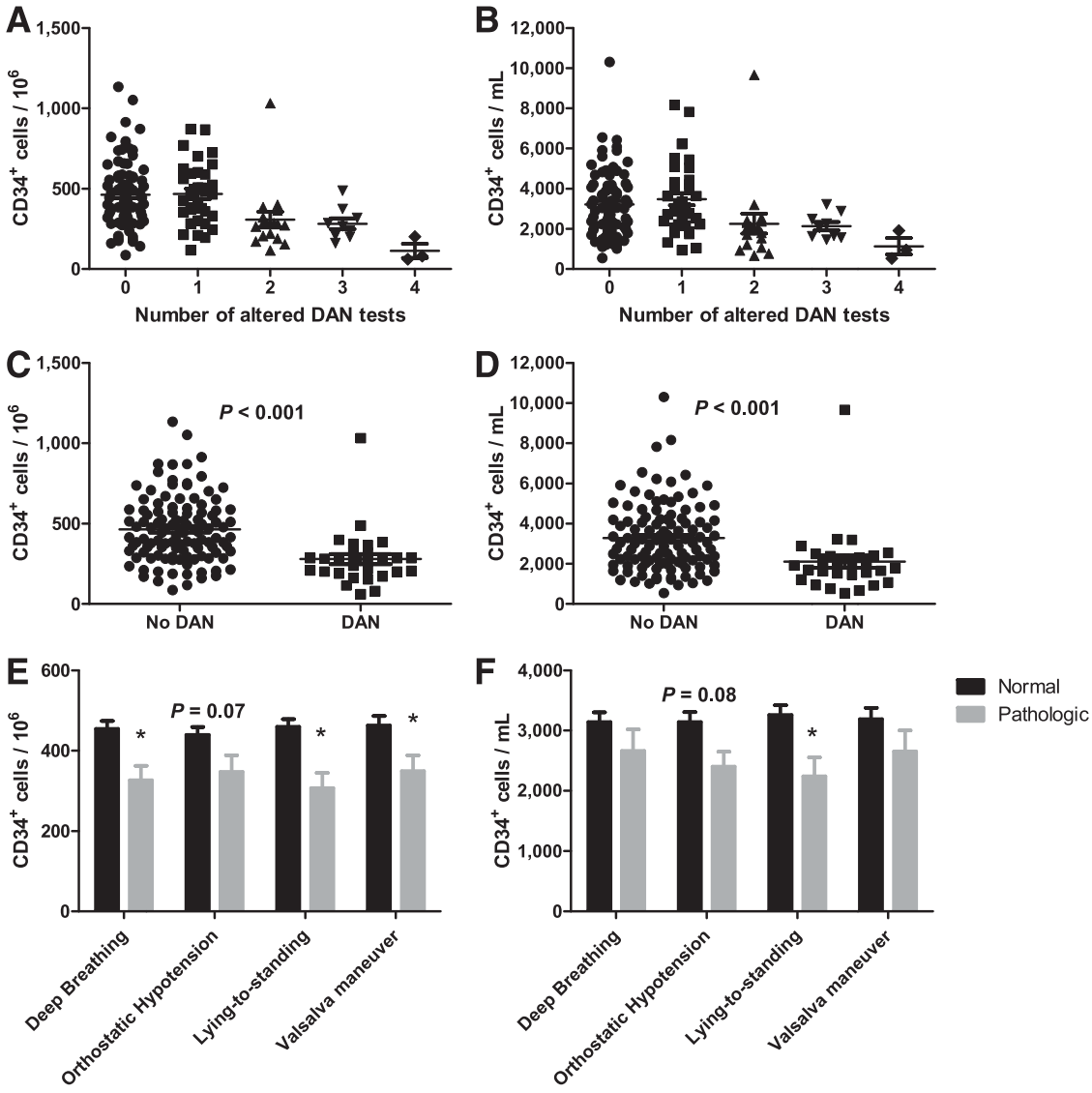

Figure 1—DAN reduces the number of circulating stem cells. *A* and *B*: Circulating CD34$^+$ cell levels (expressed as cells/10^6 events in *A* or cells/mL in *B*) are progressively reduced with increasing number of pathological DAN tests in diabetic patients. Diabetic patients meeting diagnostic criteria for DAN had reduced CD34$^+$ cells/10^6 events (*C*) and CD34$^+$ cells/mL (*D*), compared with DAN-free patients. *E* and *F*: A breakdown analysis for each DAN test showed trend reductions of CD34$^+$ cells. *$P < 0.05$, pathologic vs. normal test.

diabetic animals, while steady-state circulating levels of EPCs and LKS cells were unaffected by diabetes or sympathectomy (Supplementary Fig. 1). In vitro, STZ and 6-OHDA induced minor changes in the survival of total BM cells and CD34$^+$ BM cells, and in the generation of hematopoietic colonies (Supplementary Fig. 2). These data rule out that chemical toxicity or absolute pauperization of intramarrow stem cells account for the diabetes- and neuropathy-associated mobilopathy.

Because sympathectomy caused similar mobilization impairment as that in diabetes, we reasoned that the diabetic stem cell mobilopathy could be attributed to autonomic denervation. In support of this, we show that diabetic mice were able to mobilize LKS cells in response to AMD3100/Plerixafor (Fig. 3*C*), which is a SNS-independent mobilizer (24). In addition, the norepinephrine (NE) reuptake inhibitor desipramine, which potentiates residual SNS outflow in autonomic ganglia (25), partially restored G-CSF–induced LKS cell mobilization in diabetic mice (Fig. 3*D*).

As a functional readout of impaired mobilization after ischemia, we found that, although the microvasculature was mildly affected, hind paw perfusion was significantly impaired in diabetic and sympathectomized mice (Fig. 3*E*). This is in compliance with the known reperfusion defect of diabetes (26,27) and the recent finding that catecholamines regulate postischemic tissue remodeling (28). Collectively, these data indicate that diabetes and autonomic neuropathy hamper BM stem cell mobilization and postischemic responses.

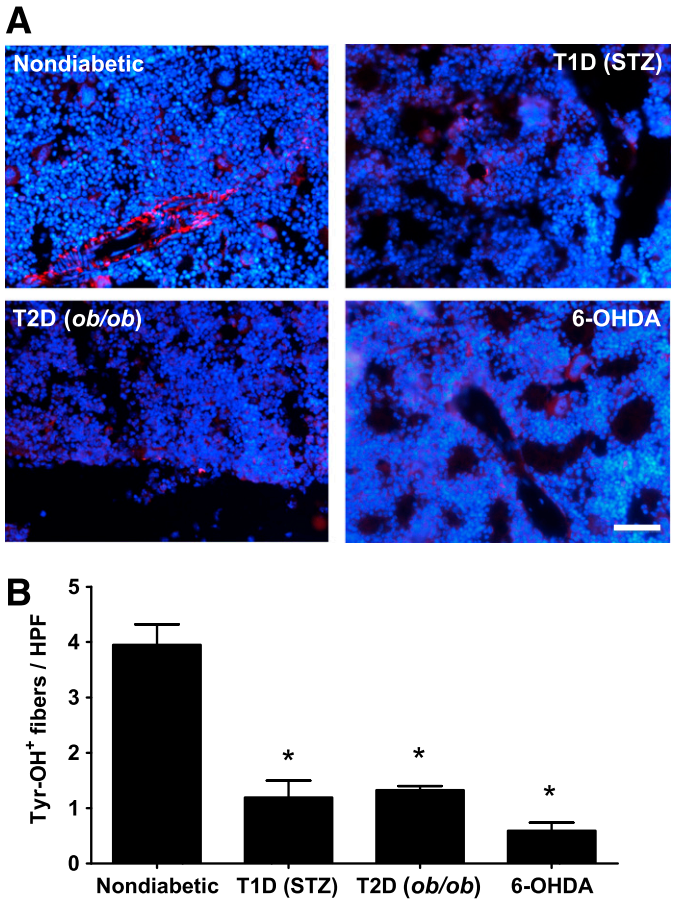

Figure 2—Experimental diabetes induces BM denervation. *A*: Representative staining of BM sections for Tyr-OH (red). Scale bar, 50 μm. *B*: Quantification of Tyr-OH staining in nondiabetic controls, T1D (by STZ administration), T2D (by crossing with *ob/ob* mice), and sympathectomized (6-OHDA) animals (n = 5/group). *$P < 0.05$.

p66Shc Mediates Diabetic BM Neuropathy

Previous studies in mice show that *p66Shc* mediates hyperglycemic damage and diabetes complications (29). Therefore, we tested whether *p66Shc* is involved in BM denervation induced by diabetes. First, we report that gene expression of *p66Shc* was increased in PBMCs of diabetic patients, which was worsened by the presence of DAN (Fig. 4*A* and Supplementary Table 2). In addition, BM cells from T1D (induced by STZ), T2D (by crossing with *ob/ob* mice), and sympathectomized (6-OHDA) mice showed increased *p66Shc* gene expression compared with controls (Fig. 4*B*). The functional consequence of this association was tested using *p66Shc*$^{-/-}$ mice, which, once made diabetic by STZ injection (T1D) or by crossing with *ob/ob* mice (T2D), were protected from BM sympathectomy, as evidenced by the preserved number of Tyr-OH^{+} fibers (Fig. 4*C* and *D*). As a result, T1D (induced by STZ) and T2D (by crossing with *ob/ob* mice) *p66Shc*$^{-/-}$ mice were able to mobilize LKS cells and EPCs after G-CSF administration, despite the fact that they were as hyperglycemic as wild-type diabetic mice (Fig. 4*E*). To confirm that restored mobilization in *p66Shc*$^{-/-}$ diabetic mice was due to preserved BM innervation, we show that STZ diabetic *p66Shc*$^{-/-}$ mice treated with 6-OHDA, which effectively denervates the BM despite *p66Shc* knockout (KO) (Fig. 4*D*), were unable to mobilize LKS cells after G-CSF stimulation (Fig. 4*F*).

Sirtuin 1 Downregulation Contributes to Impaired Stem Cell Mobilization in Diabetes

Because *Sirt1* has been implicated in EPC survival and proangiogenic activity (30), we analyzed its contribution in the mobilopathy model. We first found that *Sirt1* gene expression was reduced in PBMCs of diabetic patients with DAN compared with those without (Fig. 5*A* and Supplementary Table 2). Consistently, *Sirt1* gene expression was reduced in BM cells of T1D, T2D, and sympathectomized mice compared with controls (Fig. 5*B*). The link between neuropathy and BM *Sirt1* downregulation is strengthened by the evidence that preservation of BM innervation by *p66Shc* deletion prevented BM *Sirt1* mRNA reduction induced by T1D (by STZ administration) and T2D (by crossing with *ob/ob* mice) (Fig. 5*B*). A cAMP-dependent activation of *Sirt1* has been recently described (31), and we show here that treatment of human PBMCs with the nonselective β-adrenergic

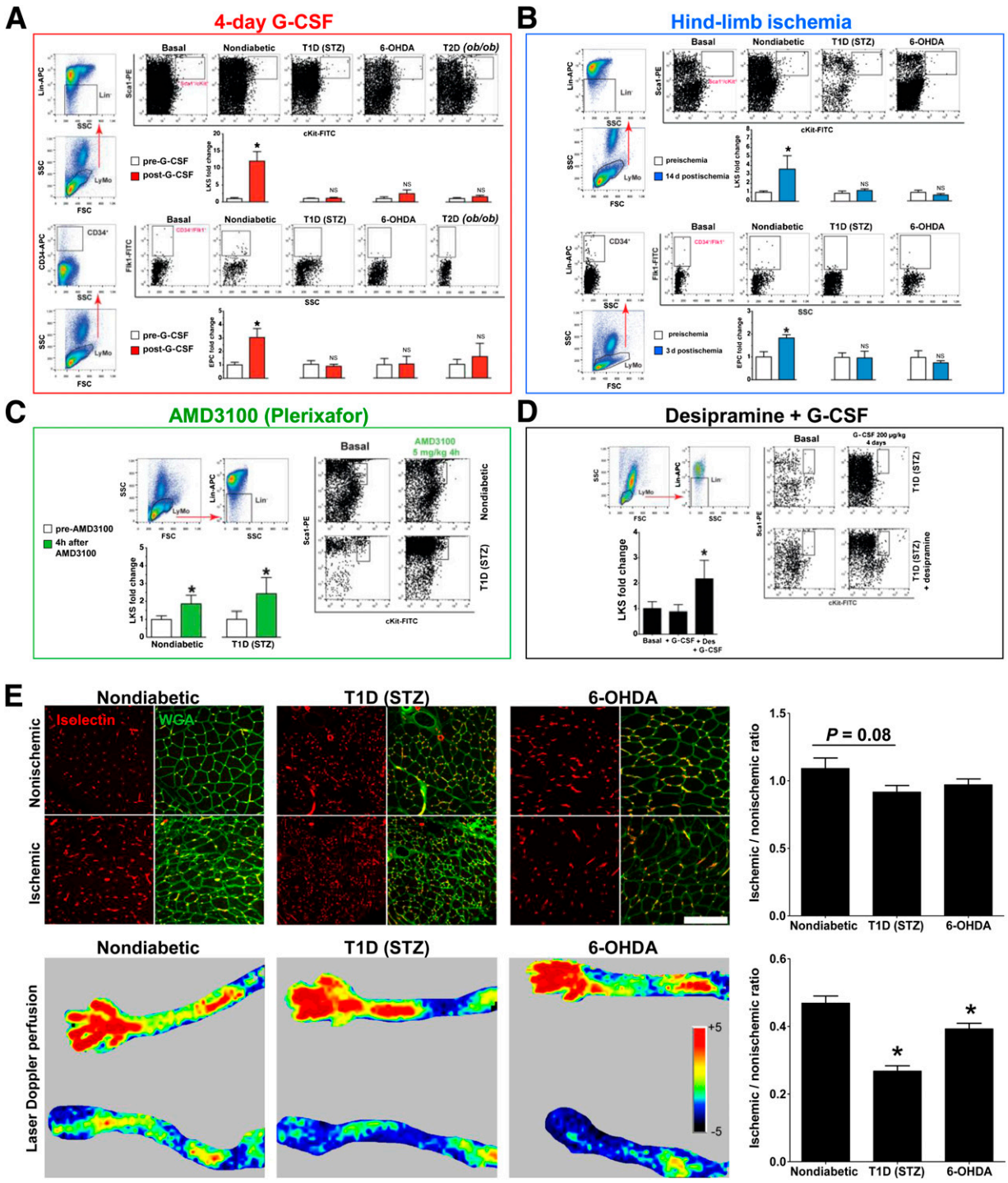

Figure 3—Impaired stem cell mobilization and ischemic response in diabetic and sympathectomized mice. *A*: Mobilization of LKS cells and EPCs after G-CSF in nondiabetic, T1D (by STZ administration), T2D (by crossing with *ob/ob* mice), and sympathectomized (6-OHDA) mice. Representative fluorescence-activated cell sorter (FACS) plots along with fold-change data are shown. **P* < 0.05 vs. pre-G-CSF (*n* = 5/group). *B*: Mobilization of LKS cells and EPCs at day 3 after hind-limb ischemia in nondiabetic, T1D (by STZ administration), T2D (by crossing with *ob/ob* mice), and sympathectomized (6-OHDA) mice. Representative FACS plots along with fold-change data are shown. **P* < 0.05 vs. preischemia (*n* = 5/group). *C*: Mobilization of LKS cell in nondiabetic and T1D (by STZ administration) mice after AMD3100 administration. Representative FACS plots and fold-change data are shown. **P* < 0.05, vs. pre-AMD3100 (*n* = 5/group). *D*: LKS cell mobilization in T1D diabetic mice after G-CSF and G-CSF + desipramine (Des). Representative FACS plots and fold-change data are shown. **P* < 0.05 vs. baseline (*n* = 3/group). *E*: Postischemic response of wild-type nondiabetic, T1D, and sympathectomized (6-OHDA) mice. Representative histological analyses of microvascular density (red, isolectin B4; green, wheat-germ agglutinin [WGA]) as well as ischemic/nonischemic ratio of the capillary/fiber density are shown. Laser Doppler quantification of paw perfusion is also reported. **P* < 0.05, vs. nondiabetic control (*n* = 5/group). SSC, side scatter; FSC, forward scatter; FITC, fluorescein isothiocyanate; Lin-APC, lineage-allophycocyanin.

agonist isoproterenol stimulated *Sirt1* mRNA expression in vitro (Supplementary Fig. 3), providing a link between sympathectomy and reduced BM *Sirt1* expression. Consistently, we also found that potentiation of NE signaling with desipramine restored *Sirt1* gene expression in the BM of T1D (by STZ administration) mice (Fig. 5*C*).

To understand the functional consequences of *Sirt1* downregulation in the BM, we generated hematopoietic-restricted *Sirt1*$^{-/-}$ mice (*Vav1-Sirt1*$^{-/-}$), lacking *Sirt1* in cells that express the *Vav1* guanine nucleotide exchange factor, which is specific for the hematopoietic system (Supplementary Fig. 4) (32). Despite the fact that inconsistent data have been reported on hematopoietic function in ubiquitous and hematopoietic *Sirt1*$^{-/-}$ mice (33,34), *Vav1-Sirt1*$^{-/-}$ mice, when subjected to G-CSF stimulation and hind-limb ischemia, recapitulated the poor mobilizer phenotype observed in diabetic and sympathectomized mice (Fig. 5*D*), supporting the idea that *Sirt1* downregulation in the BM impairs mobilization. To confirm this hypothesis, we generated *Vav1-Sirt1* transgenic (TG) mice (*Vav1-Sirt1*^{TG}), which showed a 12-fold increased expression of *Sirt1* in BM LKS cells (Supplementary Fig. 4). Once made diabetic with STZ or sympathectomized with 6-OHDA, *Vav1-Sirt1*^{TG} mice were able to mobilize LKS cells and EPCs after G-CSF and hind-limb ischemia (Fig. 5*E* and *F*), and showed improved postischemic paw perfusion (Fig. 5*G* and *H*). To test the role of *Vav1*-expressing cells in the ischemic vasculature, we analyzed *Vav1-YFP* mice, which express the yellow fluorescent protein (YFP) only in hematopoietic (Vav1^{+}) cells. Based on the integration of YFP^{+} cells into the muscle vascular endothelium of ischemic compared with nonischemic hind limbs, we show that Vav1^{+} cells can contribute to postischemic angiogenesis (Supplementary Fig. 5), explaining why modulation of *Sirt1* in Vav1^{+} cells can translate into improved recovery after ischemia. These data indicate that reduced *Sirt1* expression in the BM is responsible for the impaired stem cell mobilization in diabetic and sympathectomized mice and that this can impact on vascular recovery.

Overexpression of Adhesion Molecules Impair Stem Cell Mobilization in Diabetes and Neuropathy

Data obtained in *Vav1-Sirt1*$^{KO/TG}$ mice indicate that mobilization is affected by hematopoietic cell-intrinsic mechanisms in diabetic and sympathectomized mice. In addition, the mechanism of impaired stem cell mobilization associated with DAN are likely to be very downstream in the cascade of events that make cells leaving the niche, as is common to G-CSF and ischemia, which act on different niche components (35). Therefore, we analyzed the gene expression of a series of typical niche adhesion molecules (CD11a, CD11c, CD49d, CD49e, CD62L, and intracellular adhesion molecule 1) in BM cells, and found that they were globally upregulated in diabetic and sympathectomized mice compared with controls (Supplementary Fig. 6). The link between diabetic BM neuropathy and changes in gene expression is supported by the finding that upregulation of adhesion molecule genes occurred after the development of neuropathy in T1D mice (Supplementary Fig. 7). We focused on CD62L/L-selectin because overexpression of this molecule was previously noted by others in the diabetic BM (7). Upregulation of CD62L was confirmed by flow cytometry on LKS cells of T1D (by STZ administration), T2D (by crossing with *ob/ob* mice), sympathectomized, and *Vav1-Sirt1*$^{-/-}$ mice, whereas it was prevented in *p66Shc*$^{-/-}$ LKS cells of diabetic and sympathectomized mice (Fig. 6*A* and *B*). The link between adrenergic signaling, *Sirt1* and CD62L expression is supported by the decrease in CD62L mRNA after treatment of PBMCs with isoproterenol (Supplementary Fig. 1). L-Selectin (CD62L) is prominently involved in the trafficking of blood cells to lymphoid tissues (36), and excess L-selectin expression may render the cells more adherent to the BM stroma, preventing mobilization. The relevance of L-selectin overexpression in this setting is confirmed by the observation that genetic L-selectin deletion (*Sell*$^{-/-}$) partially restored mobilization in diabetic and sympathectomized mice (Fig. 6*C*).

DISCUSSION

This study shows for the first time that autonomic neuropathy in the BM impairs stem cell mobilization in diabetes with dysregulation of the life span–determinant genes *p66Shc* and *Sirt1*. Previous data on BM SNS in diabetes models were inconsistent, reporting either reduced (37) or increased (7) fibers. Our data indicate that T1D (by STZ administration) and T2D (by crossing with *ob/ob* mice) in mice are characterized by a profound depletion of BM SNS fibers. We also show that BM denervation in models of diabetes occurs via *p66Shc*. *p66Shc* is induced by hyperglycemia (38) and mediates the development of several complications of experimental diabetes, including cardiomyopathy (39), nephropathy (40), and delayed wound healing (41). In addition, *p66Shc* contributes to the hyperglycemic damage of BM-derived EPCs (42). Although the link between DAN and mobilopathy cannot be firmly established, the preservation of BM innervation and the rescue of mobilization in *p66Shc*$^{-/-}$ diabetic mice suggest that neuropathy impairs mobilization in models of diabetes. Other eventual effects of *p66Shc* deletion seem important in this model, because chemical denervation abolished the mobilization rescue in diabetic *p66Shc*$^{-/-}$ mice. The mobilizing activity of G-CSF is dependent on the SNS (14), and we show that hind-limb ischemia also requires a functional SNS system to elicit stem/progenitor mobilization, because it is defective in sympathectomized mice. On the other hand, AMD3100 directly disrupts the CXCR4/CXCL12 interaction to promote mobilization independently of the SNS (24). The effectiveness of AMD3100 in inducing mobilization in diabetic mice and the inefficacy of both SNS-dependent stimuli (G-CSF and

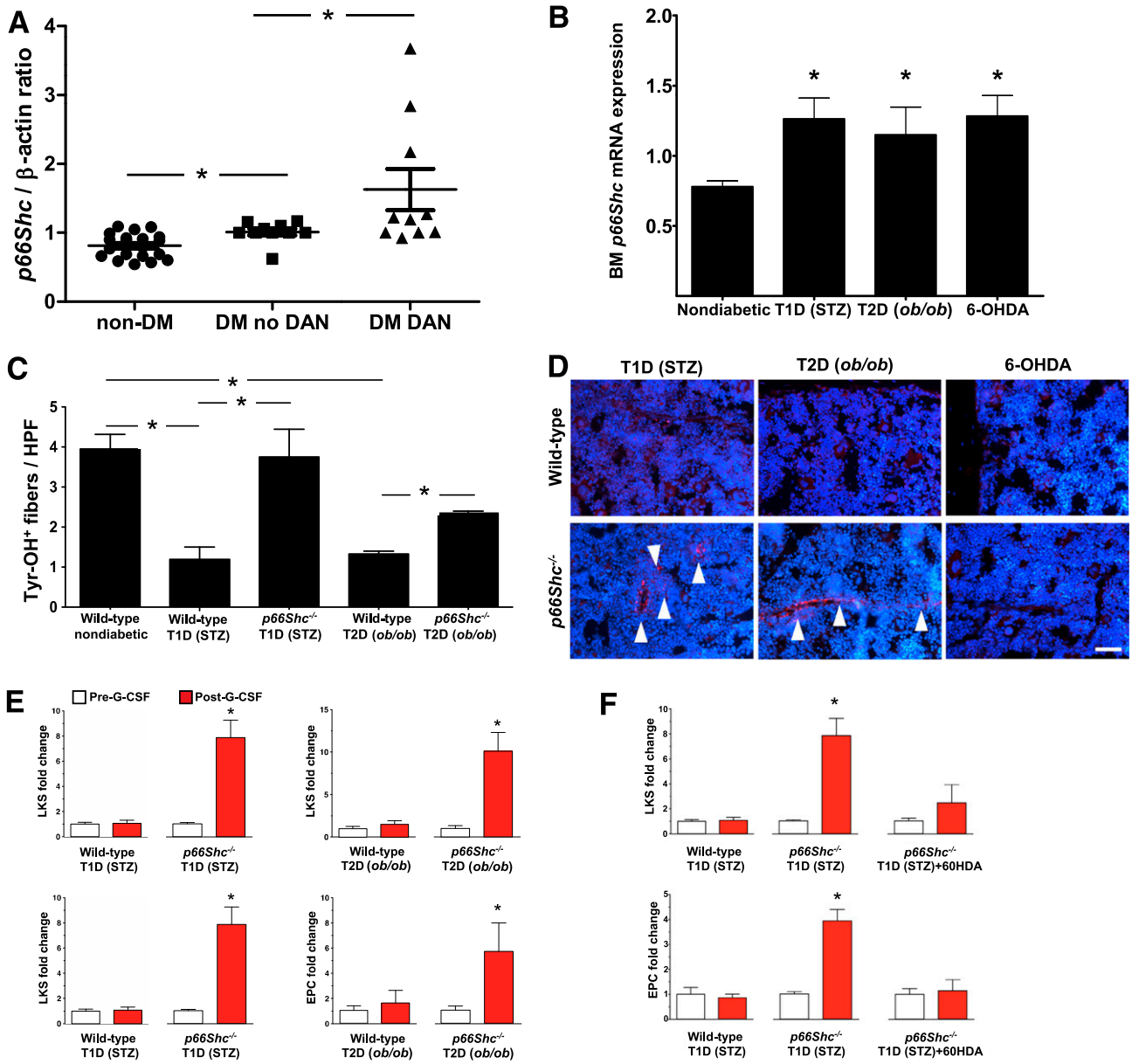

Figure 4—*p66Shc* and DAN-associated mobilopathy. *A*: *p66Shc* gene expression in PBMCs of nondiabetic individuals and diabetic patients with and without DAN. **P* < 0.05. *B*: Gene expression of *p66Shc* in the BM of control, T1D (by STZ administration), and sympathectomized (6-OHDA) mice. **P* < 0.05, vs. nondiabetic controls (*n* = 5/group). *C*: Quantification of Tyr-OH immunoreactive sympathetic fibers in wild-type and *p66Shc*$^{-/-}$ T1D and T2D mice. **P* < 0.05 (*n* = 5/group). *D*: Representative immunofluorescence images of Tyr-OH staining in control and *p66Shc*$^{-/-}$ T1D (STZ), T2D (by crossing with *ob/ob* mice), and sympathectomized mice. *E*: LKS cell and EPC mobilization in wild-type and *p66Shc*$^{-/-}$ T1D (STZ) and T2D (*ob/ob*) mice after G-CSF. **P* < 0.05, vs. baseline (*n* = 5/group). *F*: LKS cell and EPC mobilization in wild-type T1D (STZ) mice, *p66Shc*$^{-/-}$ T1D mice, and *p66Shc*$^{-/-}$ T1D 6-OHDA–treated mice after G-CSF. **P* < 0.05, vs. baseline (*n* = 3–5/group). DM, diabetes.

ischemia) are in line with the hypothesis that neuropathy impairs mobilization in diabetes. In addition, potentiation of residual SNS output by treatment with the NE reuptake inhibitor desipramine partially restored G-CSF–induced mobilization in diabetic mice. It has been demonstrated that G-CSF stimulates the SNS by reducing NE reuptake, while desipramine can rescue G-CSF–triggered mobilization in mice that mobilize poorly (25). These data suggest that a defective adrenergic signaling is responsible for impaired mobilization in diabetes and suggests a potential treatment strategy. We have previously shown that T1D and T2D patients have impaired G-CSF–induced mobilization, irrespective of the neuropathy (9). However, SNS fiber loss can be present in up to 50% of patients without clinical/instrumental evidence of DAN (43). Thus, investigation into the history and features of diabetic BM dysautonomy is an interesting matter for future research.

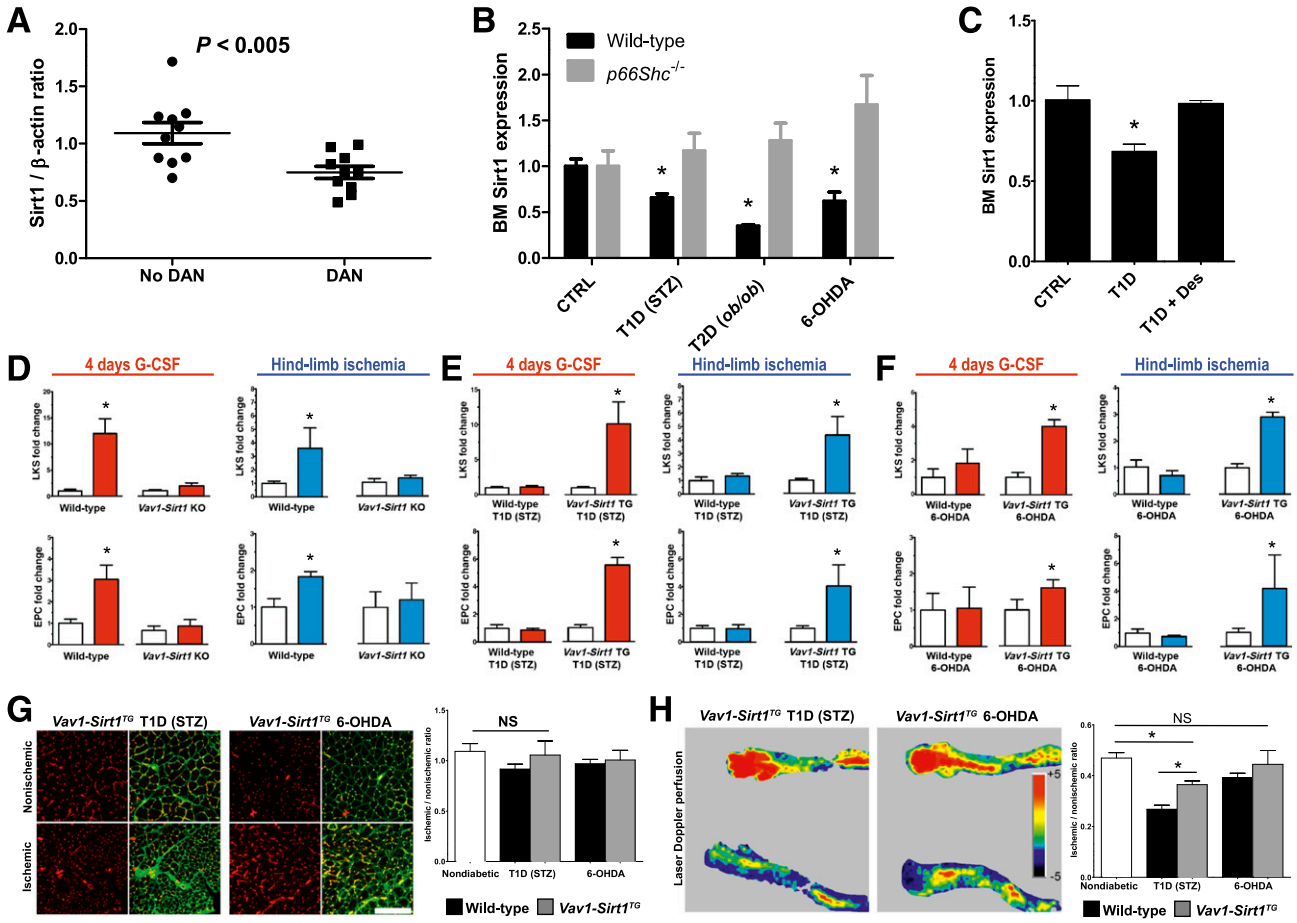

Figure 5—*Sirt1* regulates stem cell mobilization and postischemic response. *A*: *Sirt1* expression in PBMCs of diabetic patients with and without DAN. *B*: *Sirt1* expression in the BM of wild-type and *p66Shc*$^{-/-}$ nondiabetic control (CTRL), T1D (STZ), T2D (*ob/ob*) and sympathectomized (6-OHDA) mice. *$P < 0.05$ vs. controls ($n = 5$/group). *C*: BM *Sirt1* gene expression in nondiabetic controls (CTRL), T1D (STZ) mice, and T1D (STZ) mice treated with desipramine (Des). *$P < 0.05$, vs. control. *D*: LKS cell and EPC mobilization in hematopoietic-restricted (*Vav1*)-*Sirt1*$^{-/-}$ mice after G-CSF (red) and hind-limb ischemia (blue). *$P < 0.05$, post vs. pre ($n = 5$/group). *E*: LKS cell and EPC mobilization in diabetic (by STZ administration) hematopoietic-restricted (*Vav1*)-*Sirt1*–overexpressing (TG) mice after G-CSF (red) and hind-limb ischemia (blue). *$P < 0.05$, post vs. pre ($n = 5$/group). *F*: LKS cell and EPC mobilization in sympathectomized (6-OHDA) hematopoietic-restricted *Vav1-Sirt1*^{TG} mice after G-CSF (red) and hind-limb ischemia (blue). *$P < 0.05$, post vs. pre ($n = 5$/group). *G*: Postischemic response of diabetic and sympathectomized *Vav1-Sirt1*^{TG} mice compared with the respective wild-type controls. Representative histological analyses of the microvasculature (red, isolectin B4; green, laminin), as well as laser Doppler perfusion (*H*) are shown. *$P < 0.05$, vs. wild-type normal controls ($n = 5$/group).

Sirt1 has been implicated in EPC survival and proangiogenic activity (30), and its expression is reduced in EPCs of T2D patients (44) and is lowered by high glucose levels in THP-1 cells (45). Diabetic as well as chemically induced neuropathy reduced *Sirt1* expression in the BM. The mechanism whereby the SNS regulates *Sirt1* expression remains unclear, but we show that activation of the β-adrenergic receptor increases *Sirt1* mRNA in blood cells in vitro. The link between neuropathy and *Sirt1* repression is strengthened in vivo by the observation that potentiating NE signaling with desipramine rapidly restored *Sirt1* expression in the BM of T1D mice. In addition, the induction of diabetes in *p66Shc*$^{-/-}$ was not followed by *Sirt1* mRNA reduction in the BM, which can be attributed to the preserved BM innervation, although we cannot definitely rule out that metabolic dysregulations independent of neuropathy can affect *Sirt1* expression. Importantly, we show that *Sirt1* downregulation in BM cells is causally linked to impaired mobilization. In fact, hematopoietic-specific *Sirt1* KO recapitulated the poor mobilizer phenotype, while hematopoietic *Sirt1* overexpression rescued mobilization in diabetic and sympathectomized mice. As hematopoietic cell–intrinsic modulation of *Sirt1* was sufficient to influence mobilization, we focused on a series of adhesion molecules typically implicated in the trafficking of stem cells in the BM. The generalized induction of adhesion molecule genes in diabetic and sympathectomized mice, by rendering the cells more adherent to the stroma, can thus prevent mobilization. Excess CD62L (L-selectin) expression on BM LKS cells of diabetic mice was previously noted (7), and we now report that this is in fact

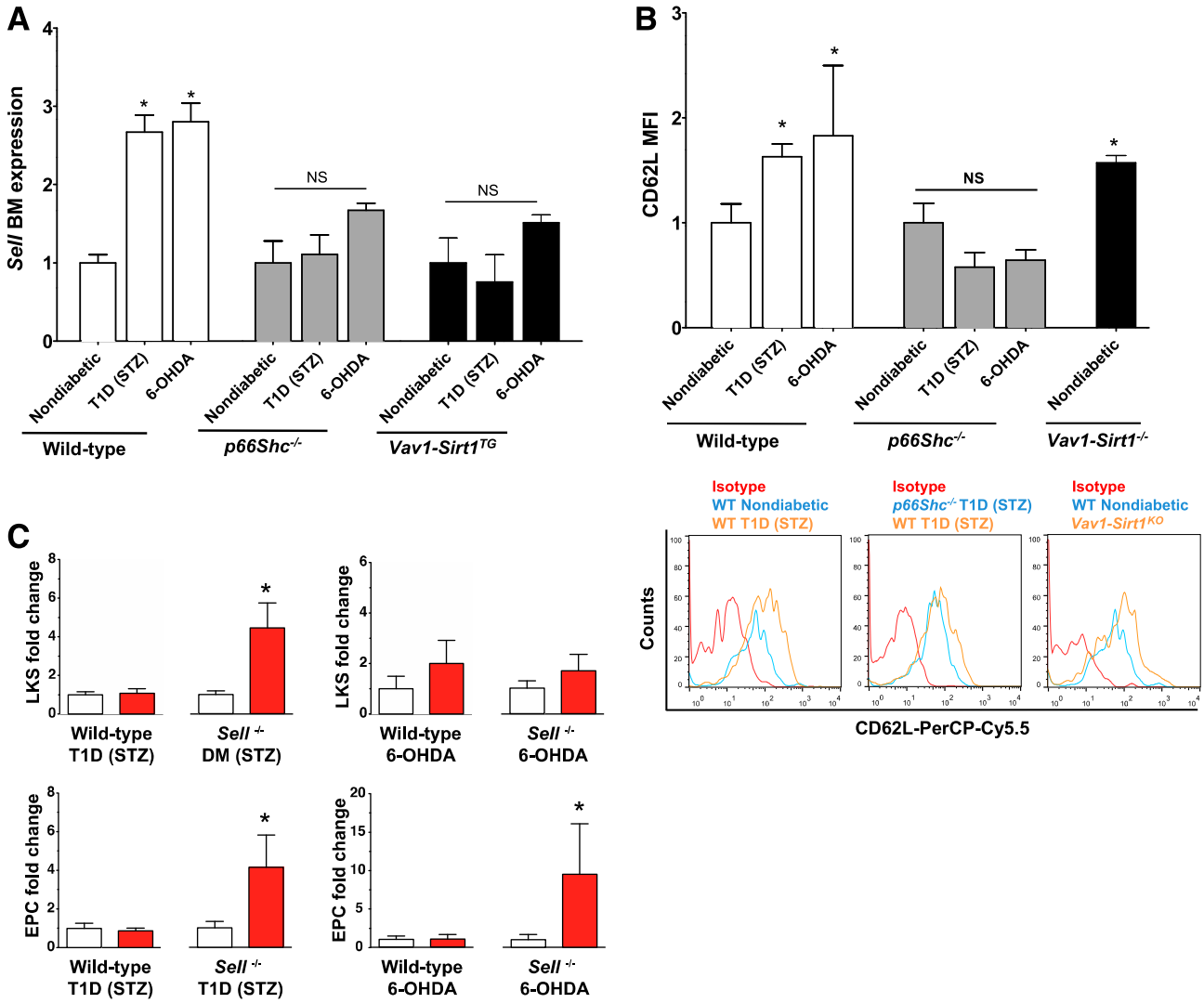

Figure 6—CD62L (L-selectin) and stem cell mobilization. *A*: BM expression of L-selectin (*Sell*) in wild-type, *p66Shc*$^{-/-}$, and *Vav1-Sirt1*^{TG} nondiabetic, T1D (by STZ administration), and sympathectomized (6-OHDA) mice. *$P < 0.05$, vs. nondiabetic. *B*: Mean fluorescence intensity (MFI) of surface CD62L expression by flow cytometry on wild-type, *p66Shc*$^{-/-}$, and *Vav1-Sirt1*$^{-/-}$ mice. *$P < 0.05$, vs. nondiabetic controls. *C*: LKS cell and EPC mobilization in L-selectin KO (*Sell*$^{-/-}$) T1D and sympathectomized mice. *$P < 0.05$, vs. baseline (n = 5/group).

implicated in the diabetes- and neuropathy-induced mobilopathy, because L-selectin deletion was sufficient to rescue mobilization in both models. Other adhesion molecules likely provide redundant signals, such that moderate increases in their expression may additively promote stem cell retention.

Together, our data suggest that BM autonomic neuropathy induced by diabetes via *p66Shc* plays a central role in the impaired BM stem cell mobilization, involving dysregulation of hematopoietic *Sirt1* and cell-intrinsic mechanisms including adhesion molecule overexpression. As multiple redundant mechanisms regulate the complex stem cell niche, it is likely that SNS-independent pathways contribute to diabetes-induced impairment in stem cell mobilization. Importantly, both in mice and in humans, diabetes induces extensive microvascular remodeling of the BM (6). We now expand this notion by showing that neuropathy is an important component of diabetic niche remodeling, with negative functional implications for mobilization.

Vascular stem/progenitor cells mobilized from the BM by G-CSF have been shown to stimulate endothelial healing and angiogenesis (46,47). In addition, ischemia-induced mobilization is considered a natural response to tissue damage that promotes angiogenesis and reperfusion (11). Therefore, impaired mobilization of cells with vasculotropic activity is expected to promote cardiovascular disease. We show that the poor mobilizer phenotype of diabetic and sympathectomized mice is associated with defective recovery after ischemia. While several

BM-independent mechanisms can contribute to this phenomenon, it is of interest that cell-intrinsic *Sirt1* overexpression rescues postischemic mobilization and reperfusion at the same time. The relevance of *Sirt1* modulation in Vav1-expressing cells is supported by the contribution played by Vav1$^+$ cells to the microvasculature of ischemic muscles. Therefore, our data suggest that the rescue of BM function in diabetes can promote recovery from ischemia.

DAN is a disabling condition with reduced life expectancy and increased cardiovascular risk (18). Our data suggest a novel possible mechanism, whereby DAN worsens vascular health. Future investigation into the features of BM neuropathy in humans and its relationships with cardiovascular DAN will shed light on this novel diabetes complication. In addition, diabetes is considered an accelerated aging disease (48), and dysregulation of longevity-determinant hubs, such as *Sirt1* and *p66Shc*, emerges as a critical factor in inducing aging features, including autonomic neuropathy, impaired stem cell mobilization, and defective recovery from ischemia. Therefore, countering aging-associated pathways has the potential to tackle vascular complications of diabetes by restoring BM function and BM-derived stem/progenitor cells.

Funding. This study was supported by LOEWE Center for Cell and Gene Therapy and SBF 834 B8/Z1 grants to M.T.; and a European Foundation for the Study of Diabetes/Lilly Grant and Fellowship Program grant and an Italian Ministry of Health grant (GR-2010-2301676) to G.P.F.

Duality of Interest. No potential conflicts of interest relevant to this article were reported.

Author Contributions. M.A. designed and performed in vivo and ex vivo experiments and contributed to manuscript writing. N.P., S.C., and G.C. performed molecular biology analyses. M.T. and R.M. generated and analyzed transgenic Vav1 mice. L.M., M.G., and P.P. generated and analyzed *p66Shc* KO mice. S.V.d.K. contributed to patient recruitment and characterization. A.A. supervised the project, provided financial support, and wrote the manuscript. G.P.F. designed the project, recruited and characterized patients, analyzed data, wrote the manuscript, and provided financial support. G.P.F. is the guarantor of this work and, as such, had full access to all the data in the study and takes responsibility for the integrity of the data and the accuracy of the data analysis.

References

1. Fadini GP, Sartore S, Agostini C, Avogaro A. Significance of endothelial progenitor cells in subjects with diabetes. Diabetes Care 2007;30:1305–1313
2. Fadini GP, Boscaro E, de Kreutzenberg S, et al. Time course and mechanisms of circulating progenitor cell reduction in the natural history of type 2 diabetes. Diabetes Care 2010;33:1097–1102
3. Fadini GP, Losordo D, Dimmeler S. Critical reevaluation of endothelial progenitor cell phenotypes for therapeutic and diagnostic use. Circ Res 2012;110:624–637
4. Oikawa A, Siragusa M, Quaini F, et al. Diabetes mellitus induces bone marrow microangiopathy. Arterioscler Thromb Vasc Biol 2010;30:498–508
5. Mangialardi G, Katare R, Oikawa A, et al. Diabetes causes bone marrow endothelial barrier dysfunction by activation of the RhoA-Rho-associated kinase signaling pathway. Arterioscler Thromb Vasc Biol 2013;33:555–564
6. Spinetti G, Cordella D, Fortunato O, et al. Global remodeling of the vascular stem cell niche in bone marrow of diabetic patients: implication of the microRNA-155/FOXO3a signaling pathway. Circ Res 2013;112:510–522
7. Ferraro F, Lymperi S, Méndez-Ferrer S, et al. Diabetes impairs hematopoietic stem cell mobilization by altering niche function. Sci Transl Med 2011;3:104ra101
8. Fadini GP, Albiero M, Seeger F, et al. Stem cell compartmentalization in diabetes and high cardiovascular risk reveals the role of DPP-4 in diabetic stem cell mobilopathy. Basic Res Cardiol 2013;108:313
9. Fadini GP, Albiero M, Vigili de Kreutzenberg S, et al. Diabetes impairs stem cell and proangiogenic cell mobilization in humans. Diabetes Care 2013;36:943–949
10. Fadini GP, Avogaro A. Diabetes impairs mobilization of stem cells for the treatment of cardiovascular disease: a meta-regression analysis. Int J Cardiol 2013;168:892–897
11. Takahashi T, Kalka C, Masuda H, et al. Ischemia- and cytokine-induced mobilization of bone marrow-derived endothelial progenitor cells for neovascularization. Nat Med 1999;5:434–438
12. Tamarat R, Silvestre JS, Le Ricousse-Roussanne S, et al. Impairment in ischemia-induced neovascularization in diabetes: bone marrow mononuclear cell dysfunction and therapeutic potential of placenta growth factor treatment. Am J Pathol 2004;164:457–466
13. DiPersio JF. Diabetic stem-cell "mobilopathy". N Engl J Med 2011;365:2536–2538
14. Katayama Y, Battista M, Kao WM, et al. Signals from the sympathetic nervous system regulate hematopoietic stem cell egress from bone marrow. Cell 2006;124:407–421
15. Spiegel A, Shivtiel S, Kalinkovich A, et al. Catecholaminergic neurotransmitters regulate migration and repopulation of immature human CD34+ cells through Wnt signaling. Nat Immunol 2007;8:1123–1131
16. Dar A, Schajnovitz A, Lapid K, et al. Rapid mobilization of hematopoietic progenitors by AMD3100 and catecholamines is mediated by CXCR4-dependent SDF-1 release from bone marrow stromal cells. Leukemia 2011;25:1286–1296
17. Lucas D, Scheiermann C, Chow A, et al. Chemotherapy-induced bone marrow nerve injury impairs hematopoietic regeneration. Nat Med 2013;19:695–703
18. Vinik AI, Ziegler D. Diabetic cardiovascular autonomic neuropathy. Circulation 2007;115:387–397
19. Hage FG, Iskandrian AE. Cardiac autonomic denervation in diabetes mellitus. Circ Cardiovasc Imaging 2011;4:79–81
20. Antonelli Incalzi R, Fuso L, Giordano A, et al. Neuroadrenergic denervation of the lung in type I diabetes mellitus complicated by autonomic neuropathy. Chest 2002;121:443–451
21. Pozzoli O, Vella P, Iaffaldano G, et al. Endothelial fate and angiogenic properties of human CD34+ progenitor cells in zebrafish. Arterioscler Thromb Vasc Biol 2011;31:1589–1597
22. Fadini GP, de Kreutzenberg S, Agostini C, et al. Low CD34+ cell count and metabolic syndrome synergistically increase the risk of adverse outcomes. Atherosclerosis 2009;207:213–219
23. Weiss RB. Streptozocin: a review of its pharmacology, efficacy, and toxicity. Cancer Treat Rep 1982;66:427–438

24. Broxmeyer HE, Orschell CM, Clapp DW, et al. Rapid mobilization of murine and human hematopoietic stem and progenitor cells with AMD3100, a CXCR4 antagonist. J Exp Med 2005;201:1307–1318
25. Lucas D, Bruns I, Battista M, et al. Norepinephrine reuptake inhibition promotes mobilization in mice: potential impact to rescue low stem cell yields. Blood 2012;119:3962–3965
26. Bento CF, Pereira P. Regulation of hypoxia-inducible factor 1 and the loss of the cellular response to hypoxia in diabetes. Diabetologia 2011;54: 1946–1956
27. Waltenberger J. Impaired collateral vessel development in diabetes: potential cellular mechanisms and therapeutic implications. Cardiovasc Res 2001;49:554–560
28. Récalde A, Richart A, Guérin C, et al. Sympathetic nervous system regulates bone marrow-derived cell egress through endothelial nitric oxide synthase activation: role in postischemic tissue remodeling. Arterioscler Thromb Vasc Biol 2012;32:643–653
29. Paneni F, Volpe M, Lüscher TF, Cosentino F. SIRT1, p66(Shc), and Set7/9 in vascular hyperglycemic memory: bringing all the strands together. Diabetes 2013;62:1800–1807
30. Zhao T, Li J, Chen AF. MicroRNA-34a induces endothelial progenitor cell senescence and impedes its angiogenesis via suppressing silent information regulator 1. Am J Physiol Endocrinol Metab 2010;299: E110–E116
31. Gerhart-Hines Z, Dominy JE Jr, Blättler SM, et al. The cAMP/PKA pathway rapidly activates SIRT1 to promote fatty acid oxidation independently of changes in NAD(+). Mol Cell 2011;44:851–863
32. Ogilvy S, Metcalf D, Gibson L, Bath ML, Harris AW, Adams JM. Promoter elements of vav drive transgene expression in vivo throughout the hematopoietic compartment. Blood 1999;94:1855–1863
33. Leko V, Varnum-Finney B, Li H, et al. SIRT1 is dispensable for function of hematopoietic stem cells in adult mice. Blood 2012;119:1856–1860
34. Singh SK, Williams CA, Klarmann K, Burkett SS, Keller JR, Oberdoerffer P. Sirt1 ablation promotes stress-induced loss of epigenetic and genomic hematopoietic stem and progenitor cell maintenance. J Exp Med 2013; 210:987–1001
35. Hoggatt J, Scadden DT. The stem cell niche: tissue physiology at a single cell level. J Clin Invest 2012;122:3029–3034
36. Ley K, Laudanna C, Cybulsky MI, Nourshargh S. Getting to the site of inflammation: the leukocyte adhesion cascade updated. Nat Rev Immunol 2007;7:678–689
37. Busik JV, Tikhonenko M, Bhatwadekar A, et al. Diabetic retinopathy is associated with bone marrow neuropathy and a depressed peripheral clock. J Exp Med 2009;206:2897–2906
38. Pagnin E, Fadini G, de Toni R, Tiengo A, Calò L, Avogaro A. Diabetes induces p66shc gene expression in human peripheral blood mononuclear cells: relationship to oxidative stress. J Clin Endocrinol Metab 2005;90: 1130–1136
39. Rota M, LeCapitaine N, Hosoda T, et al. Diabetes promotes cardiac stem cell aging and heart failure, which are prevented by deletion of the p66shc gene. Circ Res 2006;99:42–52
40. Menini S, Amadio L, Oddi G, et al. Deletion of p66Shc longevity gene protects against experimental diabetic glomerulopathy by preventing diabetes-induced oxidative stress. Diabetes 2006;55:1642–1650
41. Fadini GP, Albiero M, Menegazzo L, et al. The redox enzyme p66Shc contributes to diabetes and ischemia-induced delay in cutaneous wound healing. Diabetes 2010;59:2306–2314
42. Di Stefano V, Cencioni C, Zaccagnini G, Magenta A, Capogrossi MC, Martelli F. p66ShcA modulates oxidative stress and survival of endothelial progenitor cells in response to high glucose. Cardiovasc Res 2009;82: 421–429
43. Scholte AJ, Schuijf JD, Delgado V, et al. Cardiac autonomic neuropathy in patients with diabetes and no symptoms of coronary artery disease: comparison of ^{123}I-metaiodobenzylguanidine myocardial scintigraphy and heart rate variability. Eur J Nucl Med Mol Imaging 2010;37:1698–1705
44. Balestrieri ML, Servillo L, Esposito A, et al. Poor glycaemic control in type 2 diabetes patients reduces endothelial progenitor cell number by influencing SIRT1 signalling via platelet-activating factor receptor activation. Diabetologia 2013;56:162–172
45. de Kreutzenberg SV, Ceolotto G, Papparella I, et al. Downregulation of the longevity-associated protein sirtuin 1 in insulin resistance and metabolic syndrome: potential biochemical mechanisms. Diabetes 2010;59:1006–1015
46. Kong D, Melo LG, Gnecchi M, et al. Cytokine-induced mobilization of circulating endothelial progenitor cells enhances repair of injured arteries. Circulation 2004;110:2039–2046
47. Minamino K, Adachi Y, Okigaki M, et al. Macrophage colony-stimulating factor (M-CSF), as well as granulocyte colony-stimulating factor (G-CSF), accelerates neovascularization. Stem Cells 2005;23:347–354
48. Seshasai SR, Kaptoge S, Thompson A, et al.; Emerging Risk Factors Collaboration. Diabetes mellitus, fasting glucose, and risk of cause-specific death. N Engl J Med 2011;364:829–841